ORIGINAL RESEARCH

CrossMark

On the diagnosis of idiopathic Parkinson's disease using continuous wavelet transform complex plot

Maha Alafeef[1,2] · Mohammad Fraiwan[3]

Abstract

Gait analysis provides valuable motor deficit quantitative information about Parkinson's disease patients. Detection of gait abnormalities is key to preserving healthy mobility. The goal of this paper is to propose a novel gait analysis and continuous wavelet transform-based approach to diagnose idiopathic Parkinson's disease. First, we eliminate the noise resulting from orientation changes of test subjects by filtering the continuous wavelet transform output below 0.8 Hz. Next, we analyze the complex plot output above 0.8 Hz, which takes an ellipse, and calculate the area using 95% confidence level. We found out that this ellipse area, along with the mean continuous wavelet transform output value, and the peak of the temporal signal are excellent features for classification. Experiments using Artificial Neural Networks on the Physionet database produced an accuracy of 97.6%. Furthermore, we have shown an association between the Parkinson's disease severity stage and the ellipse complex plot area with a 97.8% overall accuracy. Based on the results, we could effectively recognize the gait patterns and distinguish apart Parkinson's disease patients with varying severity from healthy individuals.

Keywords Parkinson's disease · Vertical ground reaction force · Continuous wavelet transform · Complex plot · Diagnosis

1 Introduction and background

There are an estimated 7–10 million people living with Parkinson's disease (PD) worldwide, with the elderly being the most affected group (The Parkinson Association 2018). It is a chronic neurological disorder with no cure. Symptoms of PD progression include difficulty in controlling movement and abnormal gait patterns. Wearable devices can play an important role in all aspects of the disease, including diagnosis, monitoring, motion (i.e., Gait) data collection, and analysis (Rovini et al. 2017; Muro-de-la Herran et al. 2014; Wang 2015).

In the past few years, wearable devices have overcome many technological obstacles to reach commercial production and the mass market. Moreover, there is a continuous drive toward improving the performance of these devices in terms of power consumption, cost, speed, Internet connectivity, and functional features. This development is going hand in hand with the rise of the Internet of Things (IoT). In this context, the healthcare domain is a promising area of innovation (Li et al. 2015).

Gait signals stemming from the analysis of human locomotion provide valuable information about the PD disease diagnosis when combined with signal processing techniques (Whittle 1996). Several studies in the literature use the Fast Fourier Transform (FFT) for processing (Abdulhay et al. 2018), but this will erroneously miss many of the important features in the gait signal such as the Freezing of Gait (FOG). Moreover, the use of general gait analysis parameters (e.g., stance, swing time, and stride time) (Djuric-Jovicic et al. 2010; Perumal and Sankar 2016) may not capture the full information embedded in the gait signal, which in turn leads to the reduction in the identification accuracy.

The work addressed in this study produces a novel method to extract features using the CWT output complex plot of PD Vertical Ground Reaction Force (VGRF) gait

✉ Mohammad Fraiwan
  mafraiwan@just.edu.jo

  Maha Alafeef
  alafeef2@illinois.edu

1   Department of Bioengineering, University of Illinois
    Urbana-Champaign, Urbana, IL 61801, USA

2   Jordan University of Science and Technology, Irbid, Jordan

3   Department of Computer Engineering, Jordan University
    of Science and Technology, P.O. Box 3030, Irbid 22110,
    Jordan

signal. We show that such method has the potential not only to recognize PD but also to identify the stage progression of the disease. We investigate the relationship between PD severity and the extracted features. The contributions of this paper are as follows:

1. We analyze the VGRF using the continuous wavelet transform (CWT) and identify the energy complex plot of the CWT as an indicative and efficient classification feature for the identification of PD patients.
2. We identify the severity level of PD using the same features, which is a first in the literature to the best of our knowledge.
3. We build a classification model using the proposed features and Artificial Neural Networks (ANN).
4. We evaluate the performance of the system and report a PD identification accuracy of 97.6%, and a severity level recognition overall accuracy of 97.8%.

The rest of the paper is organized as follows. In section 2 we survey the related work in the literature and its methods. In Sect. 3 we present our methodology, data acquisition, theoretical framework, and data analysis. Section 4 discusses the data classification results. We conclude in Sect. 5.

2 Related work

The IoT, empowered by the tremendous development in wearable devices, provides a framework for the development of connected pervasive applications. A layering of service, devices, and communication modules allows us to focus on the specific research problems on hand. In this context, Wang (2015) discussed the rising importance of health monitoring devices to the older disease-prone section of society, and introduced an architecture design for the deployment of health monitoring sensors. Moreover, the issues of data communication and security are of prime importance (Zhu and Yang 2015). Such studies facilitate the deployment of the work in this paper.

Artificial Intelligence (AI) and machine learning plays a paramount role in automating many of the human-dependent processes. The performance of these methods is continuously undergoing evaluation and refinement in the face of challenges emerging from Big Data and the IoT (Ngia and Sjoberg 2000; Lera and Pinzolas 2002; Kermani et al. 2005; Arridha et al. 2017).

The importance of PD early diagnosis and disease progression identification should not be underestimated (Hoehn et al. 1998). To this end, the Movement Disorder Society (MDS) has been conducting regular reviews of the Unified PD Rating Scale (UPDRS) to better reflect the disease progression across different genders and races, which is also emphasized by the work of Hoehn et al. (1998). The disease is affecting Millions of people worldwide and technology can play a major role in the disease management.

Gait analysis plays an important role in studying and quantifying the motion process in a non-invasive manner. It is useful for the assessment of many ailments including chronic heart conditions (e.g., Congestive heart failure), lung diseases [e.g., Chronic obstructive pulmonary disease (COPD)] (Juen et al. 2014), Autism (Weiss et al. 2013), and neurodegenerative diseases (e.g., Huntington and Amyotrophic Lateral Sclerosis) (Prabhu et al. 2018).

Abnormal motion maybe a symptom of serious disorders, as exemplified by PD patients. Wearable sensors, coupled with cameras and observation, measure the muscular activity, force exerted by the feet, and body mechanics (Chester et al. 2005; Muro-de-la Herran et al. 2014). By analyzing abnormal values of gait parameters, it is possible to identify disorders as well as the PD disease stage progression. Moreover, it can be used to assess the efficacy of the therapeutic process and medication, and guide the disease management plan. For example, Deep brain stimulation is an emerging technique for PD treatment. The efficiency of this method is assessed by monitoring changes in the patient gait, because the treatment is reflected on the patients motor system (Hadoush et al. 2018; Lattari et al. 2017; Fregni et al. 2006).

Several artificial intelligence and signal processing techniques have been used to build automated PD diagnostic systems based on gait analysis. These methods rely on extracting certain features and markers of PD. Fraiwan et al. (2016) developed a smartphone application to measure the hand tremors of PD patients using the embedded accelerometer. The data was analyzed using two level wavelet packets and the extracted features were classified using a neural networks classifier.

In another avenue of the literature, Vertical Ground Reaction Force (VGRF) data has been used as a marker of PD. Such data is obtained from sensors (e.g., accelerometers and gyroscopes attached to the feet (Tadano et al. 2013; Tao et al. 2012) or embedded in the insoles of the shoes (Alam et al. 2017). The goal was to study the movement characteristics of PD patients as compared to healthy individuals, extract features, and classify the data into normal or PD. Abdulhay et al. (2018) analyzed features like stance, stride time and swing time to highlight the duration of the pulse and peak. Then, the features were used to distinguish PD from normal gait patterns using Medium Gaussian Support Vector Machine (SVM). Similarly, Manap et al. (2011) fed kinematic and kinetic features, among others, to Artificial Neural Networks (ANN) to classify healthy and PD gait values. The work of Alam et al. (2017) extracted features from PD gaits signals using the coefficient of variation (CV) of stride time and swing time, along with the standard deviation and mean of the force center of pressure. They compared the

performance of four classification algorithms; SVM, decision trees, K-nearest neighbor, and random forest. The SVM with cubic kernel was found to be of the best performance in terms of accuracy.

Lee and Lim (2012) used wavelet transform for feature extraction. Three signal combinations were calculated and then the wavelet transform was applied to produce approximation and detail coefficients. Forty features were extracted from these coefficients via statistical methods (e.g., frequency distributions and variability). For classification, a neural network with weighted fuzzy membership functions was used. Djuric-Jovicic et al. (2010) recorded gait kinematics with a wireless inertial measurement system along with video recording. The Freezing of Gait (FOG) was identified by Medical experts. They used Simple signal processing algorithm combined with perception neural network and rule-based classification to validate the results.

3 Material and methods

Figure 1 shows the method used to build the classification model. It consists of the following steps:

1. Compute the CWT of the gait signal as obtained from the vertical ground reaction force (VGRF). This results in a function of both time and frequency. The output is complex values (i.e., the mother wavelet is a complex function).
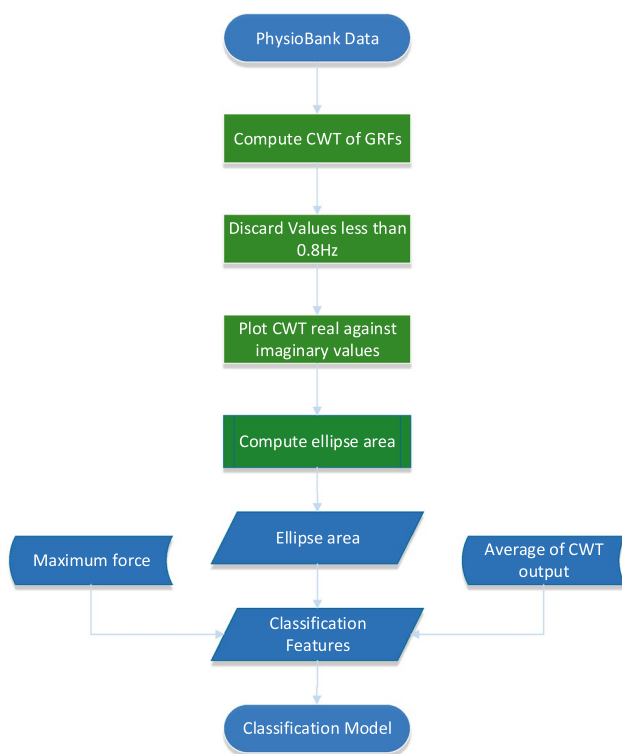2. Discard the output pertaining to the frequency values less than 0.8 Hz. This eliminates the noise resulting from the subjects body orientation changes.
3. Construct the wavelet energy complex plot of the CWT output real part against the imaginary one.
4. For all the signals from the 16 sensors, and the sum signals of all sensors for each foot:
   (a) Compute the ellipse area of the complex plot with 95% confidence. This is the first feature for classification.
5. Compute the average wavelet energy associated with frequency higher than 0.8 Hz, and the maximum force exerted in every sensor. These will serve as two more features for classification.
6. Build the classification model using the features, in steps 4 and 5 above, and the artificial neural network (ANN) model.

Next, we go through the details about the dataset, continuous wavelet transform, ellipse area computing, features calculation, classification, and performance evaluation.

3.1 Data acquisition

The data was downloaded from PhysioBank (PhysioNet 2018) as recorded by Yogev et al. (2005). It contained VGRF recordings from 73 healthy controls and 93 idiopathic PD subjects (35 women and 58 men, mean age 66.3 years) and (33 women and 40 men, mean age 63.7 years). Each PD record is assigned a Hoehn and Yahr and/or the UPDRS score. The PD patients involved in this study were diagnosed with moderate disease severity or at the early stage of the disease development. Out of the 93 idiopathic PD subjects, 38 are of intermediate disease severity (10 subjects have Hoehn and Yahr score 3, and 28 with Hoehn and Yahr score 2.5). The other 55 PD patients are belonging to early stage category with Hoehn and Yahr score 2. The gait signal was recorded using eight different force sensors located in the insole of both feet of the subjects. The sensors measured the VGRF in Newtons as a function of time while the subjects were walking for about 2 min on a level ground and a self-selected path. Moreover, two more signals produced by the sum of the eight sensor outputs from each foot were used. Thus, we have 18 overall signals for every subject. The individual output of these 16 force sensors was digitized at a sampling frequency of 100 Hz. In addition to minimizing the startup and end up effects, the first 20 s and last 10 s of the gait signal were already excluded in this dataset. Also, a median filter was applied to the recorded data for outliers data points removal. Thus, the effect of movement energy variation on gait motion is minimized for the sake of precise feature

Fig. 1 The method of building the classification model

computation. This leads to an accurate representation of gait dynamics and characteristics.

3.2 Continuous wavelet transform

Several fields in communication, biomedical, and signal processing use CWT to analyze signals in the time-frequency domain (Qiao et al. 1998). The time-frequency feature of wavelet transform gives descriptive information about the signal distribution with respect to the frequency for every point in time. To analyze a signal, two types of wavelet transformation can be used; CWT and discrete wavelet transform (DWT). In the present study, using CWT allows us to consider the signal in the combined time and frequency domains. The CWT of a signal $x(t)$ is defined as:

$$CWT(a,b) = \int x(t)\psi_{a,b}(t)dt \tag{1}$$

where:

$$\psi_{a,b}(t) = \frac{1}{\sqrt{|a|}}\psi\left(\frac{t-b}{a}\right) \tag{2}$$

$\psi(t)$ is known as the mother wavelet and $\psi_{a,b}(t)$ is the dilation and transformation of $\psi(t)$, b is a time shifting parameter that captures the time domain characteristics of the signal $x(t)$. a is a scaling parameter, which provides the mother wavelet function $\psi(t)$ dilation and compression characteristics. The entire frequency range is covered by choosing the scaling parameter based on the following formula:

$$f = \frac{f_c}{aT_s} \tag{3}$$

where T_s is the sampling period and f_c is the mother wavelet center frequency.

We used analytic Morse wavelet as the mother wavelet. The shape and transformation behavior of this wavelet is affected by the symmetry (γ) and time-bandwidth (ρ) parameters. The γ parameter controls the wavelet function symmetry in time based on the demodulate skewness; whereas the time-bandwidth parameter (ρ) determines the wavelet time duration (Lilly and Olhede 2009; Olhede and Walden 2002). Moreover, the peak frequency is related to γ and ρ, as follows:

$$Peak\ frequency = \left(\frac{\rho^2}{\gamma}\right)^{\frac{1}{\gamma}} \tag{4}$$

The duration determines the number of oscillations at peak frequency that can fit into the time-domain wavelet's center window. Thus, to increase the number of wavelet oscillations under the filter, we chose ρ to be 60. Moreover, γ was chosen to be 3 because this value leads to 0 skewness of the Morse

wavelet, while having a minimum Heisenberg area (Lilly and Olhede 2012; MathWorks 2018).

3.3 CWT energy complex plot and the ellipse area

As confirmed by the results, the complex plot (CP) of the wavelet energy represents an effective and indicative classification feature for the diagnosis of idiopathic PD from healthy gait signals. The CP of signal $x(n)$ is obtained by plotting the real part of the signal $R(n)$ against the imaginary part, $IM(n)$. As indicated earlier, the wavelet energy from the CWT of the gait signal, with the frequency content higher than 0.8 Hz, was used for the calculation. Thus, the complex plot is a graphical representation of magnitude and phase of wavelet energy distribution for the frequency higher than 0.8 Hz associated with every time point.

The wavelet energy complex plot takes an ellipse shape (see Fig. 4). This motivated us to compute its area. A 95% confidence method has been used for ellipse area computation (Thuraisingham et al. 2007; Pachori et al. 2009; Cavalheiro et al. 2009). The method covers 95% of the CP points. The ellipse area measured from the wavelet complex plot was computed for every sensor as a feature set for classification. The procedure for the ellipse area calculation with 95% confidence is as follows (Cavalheiro et al. 2009; Prieto et al. 1996):

1. Compute the average values of $R(n)$ and $IM(n)$ as:

$$m_R = \sqrt{\frac{1}{N}\sum_{n=0}^{N-1}R^2(n)} \tag{5}$$

$$m_{IM} = \sqrt{\frac{1}{N}\sum_{n=0}^{N-1}IM^2(n)} \tag{6}$$

$$m_{R,IM} = \frac{1}{N}\sum R(n)IM(n) \tag{7}$$

2. Compute parameter D as:

$$D = \sqrt{m_R^2 + m_{IM}^2 - 4(m_R^2 m_{IM}^2 - m_{R,IM}^2)} \tag{8}$$

$$a = 1.7321\sqrt{m_R^2 + m_{IM}^2 + D} \tag{9}$$

$$b = 1.7321\sqrt{m_R^2 + m_{IM}^2 - D} \tag{10}$$

3. Calculate the ellipse area as:

$$Area = \pi ab \tag{11}$$

3.4 Gait VGRF features

Three features from the CWT analysis have been utilized for the classification; the ellipse, averaged energy and peak amplitude of the gait signal. The data was divided randomly into 70% for training and 30% for validation and testing. Supervised learning was conducted using the Levenberg–Marquardt learning function. Table 1 shows the average and standard deviation of the three features. In general, they are higher for normal subjects as opposed to patients diagnosed with PD. These differences in the feature space vectors can be used as an indicator of the degeneration of the motor system responsible for regulating the human movement.

3.5 Machine learning model

Artificial neural networks (ANN) are commonly used for pattern recognition problems (Krogh 2008; Partridge et al. 1999). In this work, a neural network with one hidden layer was used for building the machine learning model. The ANN is a network consisting of processing units called neurons, which are comprised of three layers; Input layer, hidden layer, and output layer. Each neuron connection has a weight that represents the learnt knowledge through training (Okut et al. 2011; Felipe et al. 2014; Svozil et al. 1997; Lweesy et al. 2011). The input propagates through the various layers for processing, and the classification results are obtained from the output layer. Moreover, all of the neurons in the hidden layer connected with those in the output layers via bias values which represent the threshold value for neuron activation (Svozil et al. 1997).

The activation (output) value, X_i, of the ith neuron is defined in terms of the the potential ε_i and transfer function $f(\varepsilon_i)$ as:

$$X_i = f(\varepsilon_i) \tag{12}$$

$$\varepsilon_i = -\partial_i + \sum_{j=1} X_i W_{ij} \tag{13}$$

$$f(\varepsilon_i) = \frac{1}{1 + e^{-\varepsilon}} \tag{14}$$

Table 1 Average and standard deviation of the extracted values of the proposed features

	Normal		PD	
	Mean	Std dev	Mean	Std dev
Ellipse area	190916.3	194591.5	122954.6	156357.3
Mean of wavelet energy	59.07	33.06	53.92	34.43
Peak of wavelet energy	381.74	105.38	359.12	98.28

The network modifies itself through supervised training to adjust the connection weights w_{ij} and the threshold coefficients f_{ij} in an iterative manner with the goal of reaching the minimum square difference (E) between the computed and the targeted output, as follows:

$$E = \sum_o \frac{y - \hat{y}}{2} \tag{15}$$

where y_o is the computed training output and $\hat{y}_o$ is the targeted output.

3.6 Performance evaluation

To evaluate the performance of the proposed method, we used the commonly used parameters in the literature; accuracy, sensitivity, and specificity defined as:

$$accuracy = \frac{TP + TN}{TP + TN + FN + FP} \times 100\% \tag{16}$$

$$sensitivity = \frac{TP}{FN + TP} \times 100\% \tag{17}$$

$$specifity = \frac{TN}{TN + FP} \times 100\% \tag{18}$$

where TP the number of instances correctly classified as PD. TN the number of instances correctly classified as normal. FP the number of misclassified PD cases. FN the number of misclassified normal subjects.

4 Results and discussion

Utilizing spectral features for PD classification combined with temporal features provides a new insight into using PD VGRF signals to analyze the disease state and severity. The time-frequency analysis gives new information, which cannot be inferred from the original time-series. The frequency distribution of gait cycle plot as function of time give us the means to differentiate between PD and normal subjects, see Figs. 2 and 3. We found that the maximum power amplitude is concentrated in the frequency range of 0.8–1 Hz for almost all time points. However, this peak amplitude is higher in normal subjects compared with PD subjects as normal healthy subjects exert higher force at 0.8–1 Hz. It can be observed that there are short high energy segments in the normal subject scalogram around 0.8–1 Hz. whereas, the PD scalogram shows longer high energy segments compared to healthy subjects. This can be related to the fact that the
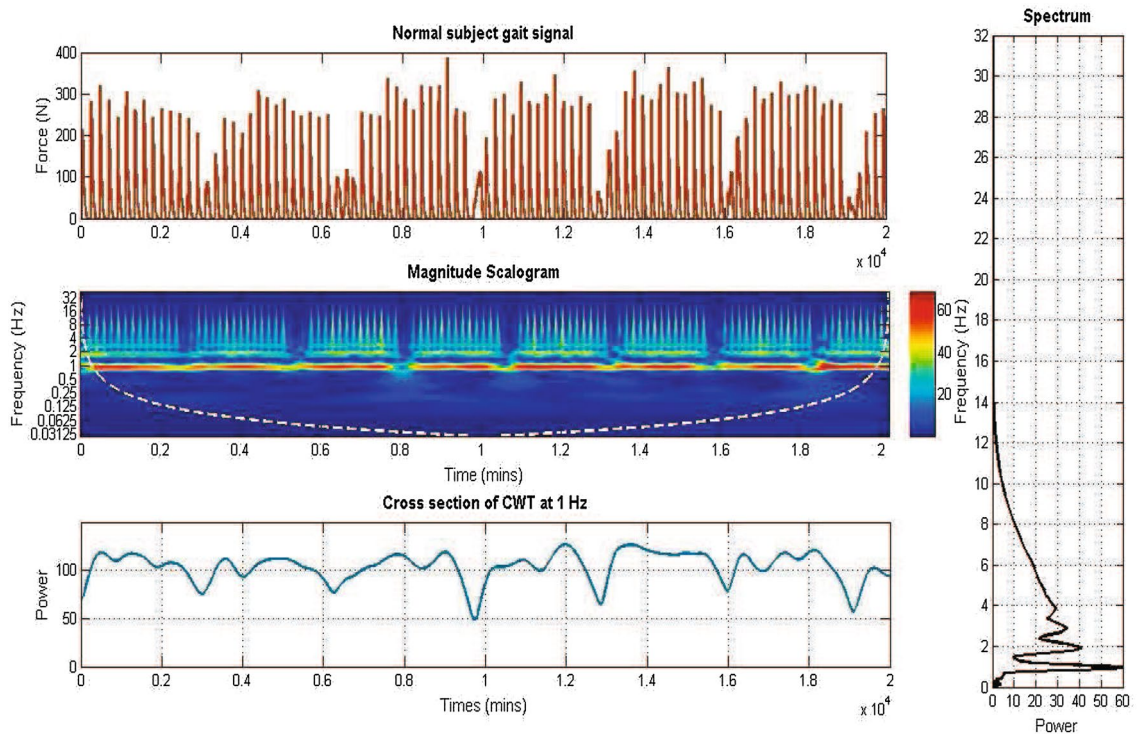
Fig. 2 Normal gait signal, its related scalogram, cross section at 1 Hz as function of time, and the spectrum of the normal gait signal at 1.2 min
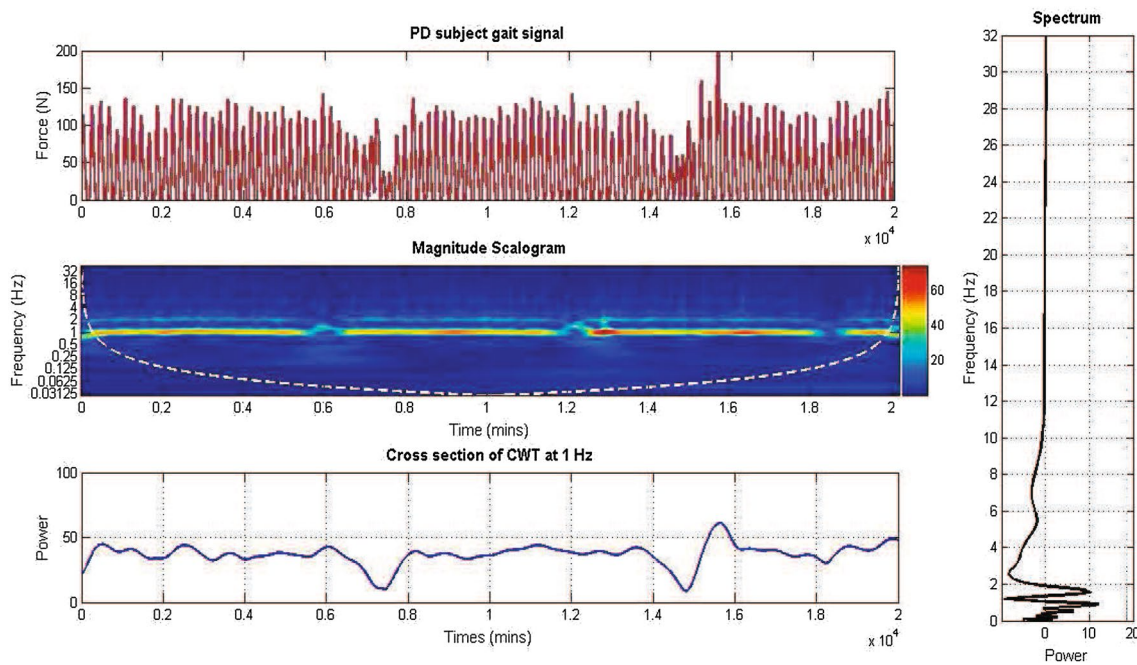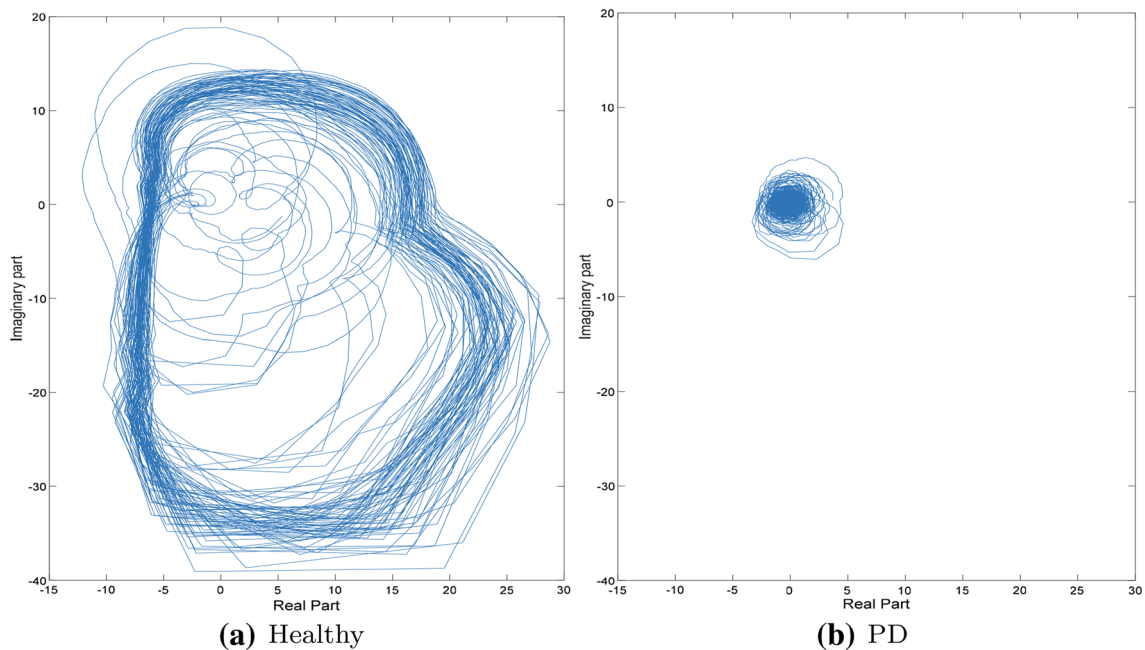

Fig. 3 PD gait signal, its related scalogram, cross section at 1 Hz as function of time, and the spectrum of the PD gait signal at 1.2 min

(a) Healthy   **(b)** PD

Fig. 4 The complex plot of normal gait and PD subject. It is clear that the ellipse area of wavelet complex plot greater for healthy subjects as compared with PD subjects

healthy gait cycle has 3:2 stance to swing time ratio. However, this is not the case in PD subjects as they experience more friction for longer time while walking.
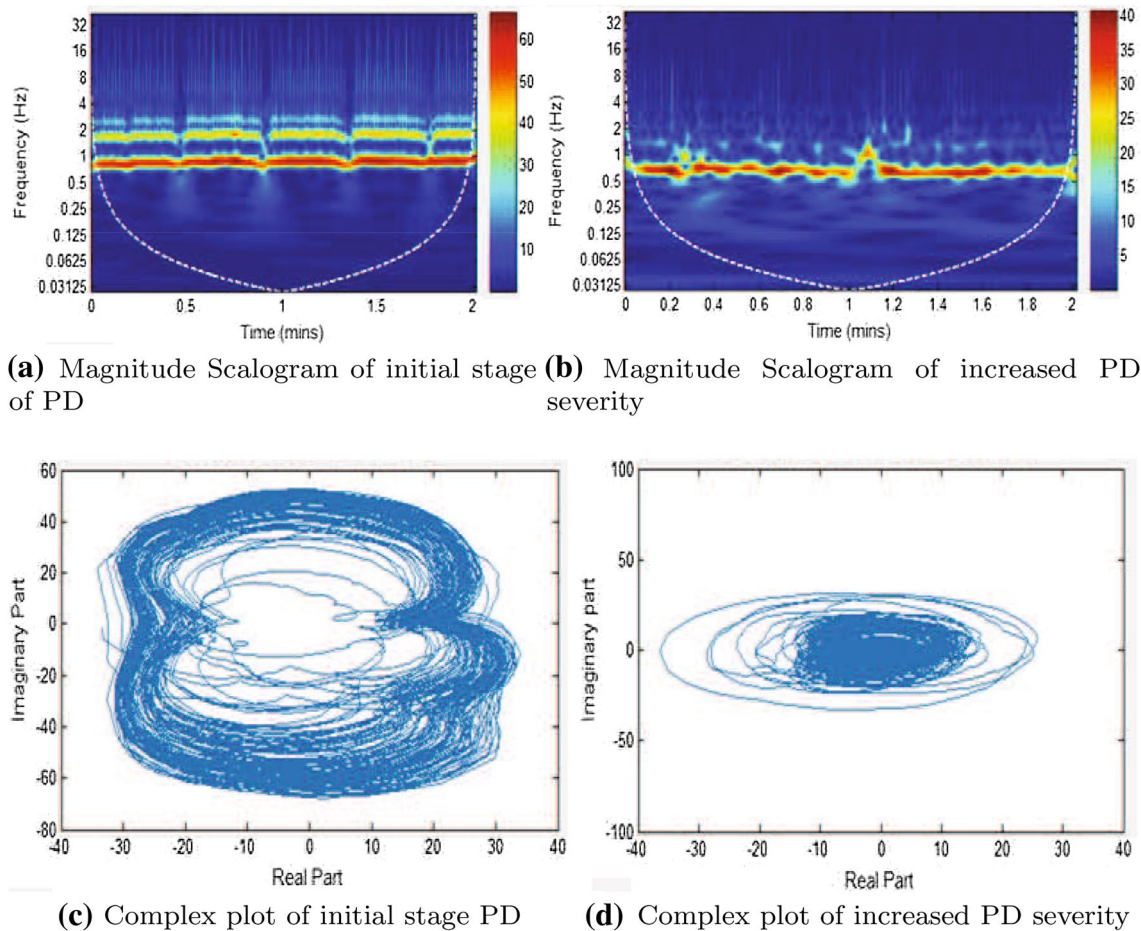
The wavelet energy complex plot of both PD and normal subject takes an ellipse shape with the higher area occupied by the normal subjects, see Figs. 4 and 5. From the analysis results, it can be observed that the ellipse area of the complex plot is large for normal subjects and decreases significantly as the PD severity level increases. Thus, the area can be used as an indicator for PD severity stage and provides a method for distinguishing between normal and PD subjects in the early stage. Further, the high amplitude segments occurred around 1Hz are observed to be shorter in early stage PD and longer in high PD severity.

Figure 6, the 3D view of the complex plot as function of time, shows significant differences between PD and healthy subjects in terms of the wavelet energy values behavior as it goes forward in time. The normal healthy subject has a regular circular pattern as function of time, as it converges smoothly and regularly toward the helix center for all time

points. Thus, we have regular phase (imaginary component values) as function of time (Fig. 6a). Whereas, the PD subjects exhibit an irregular pattern of complex plot as function of time with no smooth transition (Fig. 6b). This is caused by the instable pattern present in the PD gait signal compared to normal stable signal.

The inclusion of both spectral and temporal features extracted from VGRF signals led to the ability to diagnose PD subject from normal ones with 97.6% overall accuracy. The training accuracy was 99.1% and the validation+testing accuracy was 94%. The specificity and sensitivity were 97.14% and 86.67% respectively. The number of FP cases was 2, which is the same number for the FN. In comparison to other studies of the same dataset (Abdulhay et al. 2018; Bakar et al. 2012; Djuric-Jovicic et al. 2010; Perumal and Sankar 2016; Zhang et al. 2013), utilizing the CWT and the complex plot improved the classification accuracy by at least 4.9% as shown in Fig. 7.

The model was able to distinguish the severity level, based on the Hoehn and Yahr scale, with testing and overall

(a) Magnitude Scalogram of initial stage of PD

(b) Magnitude Scalogram of increased PD severity

(c) Complex plot of initial stage PD

(d) Complex plot of increased PD severity

Fig. 5 The scalogram and the complex plot of wavelet energy associated with initial PD and increased severity PD subject. The ellipse area decreases as the PD severity increases
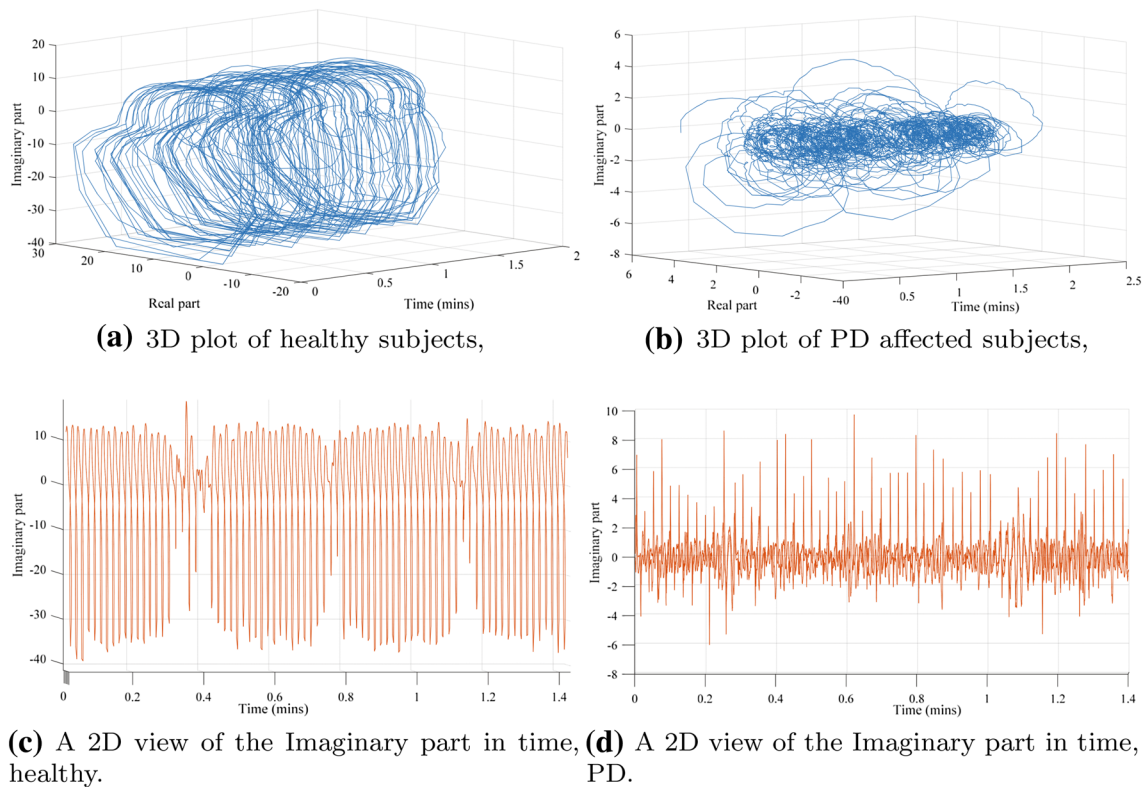
accuracies of 96.7% and 97.8% respectively. Moreover, the training accuracy was 100% and the combined testing and validation accuracy was 95.1%. The number of FP and FN cases was 1 each. The sensitivity was 98.8% and the specifity was 90.0%.

5 Conclusion

In this paper, the ellipse area resulting from the CWT energy complex plot of VGRF data was investigated as a potential feature for the identification and classification of

PD patients from normal subjects. The method was evaluated on a publically available and commonly used dataset, and the results outperformed existing literature. This confirms the efficacy of the proposed method. Overall, we believe that features extracted from the gait signal spectral analysis supported by temporal feature has the potential to improve the diagnosis and monitoring processes. The force signal time-frequency profile provided an efficient way of distinguishing a healthy person from a PD subject. Moreover, the ellipse area was found to be sensitive to the PD severity stage. Hence, it can provide great aid in early PD diagnosis.

(a) 3D plot of healthy subjects,

(b) 3D plot of PD affected subjects,

(c) A 2D view of the Imaginary part in time, healthy.

(d) A 2D view of the Imaginary part in time, PD.

Fig. 6 3D plot of wavelet energy real and imaginary parts as a function of time. In **a** the loop converges and shows a stable pattern while in **b** there is an unstable pattern, which changes its shape at different time points

Fig. 7 Accuracy comparison of our approach to other related studies
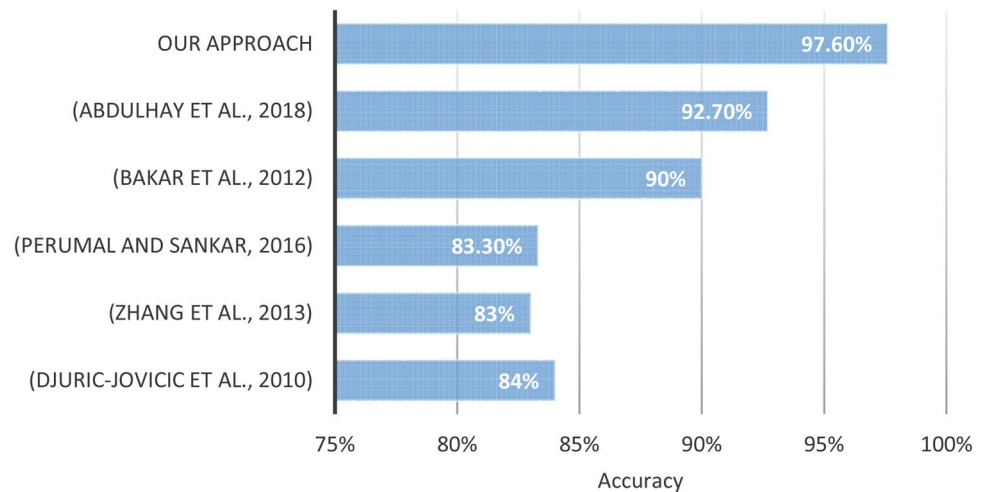
In future work, VGRF data will be further analyzed to find methods of extracting more information about the PD stage identification, and the fusion of more features into the classification model to improve the classification accuracy.

For example, using the spectral-derived features combined with temporal features opens a new avenue for gait signal analysis using stability plots.

References

Arridha R, Sukaridhoto S, Pramadihanto D, Funabiki N (2017) Classification extension based on IOT-big data analytic for smart environment monitoring and analytic in real-time system. Int J Space Based Situat Comput 7(2):82–93. https://doi.org/10.1504/IJSSC.2017.086821

Abdulhay E, Arunkumar N, Narasimhan K, Vellaiappan E, Venkatraman V (2018) Gait and tremor investigation using machine learning techniques for the diagnosis of Parkinson disease. Future Gener Comput Syst. https://doi.org/10.1016/j.future.2018.02.009 (ISSN 0167-739X)

Alam MN, Garg A, Munia TT, Fazel-Rezai R, Tavakolian K (2017) Vertical ground reaction force marker for Parkinsons disease. PLOS One 12(5):e0175951. https://doi.org/10.1371/journal.pone.0175951

Bakar ZA, Ispawi DI, Ibrahim NF, Tahir NM (2012) Classification of Parkinson's disease based on multilayer perceptrons (MLPS) neural network and ANOVA as a feature extraction. In: 2012 IEEE 8th international colloquium on signal processing and its applications, Melaka, Malaysia, pp 63–67. https://doi.org/10.1109/CSPA.2012.6194692

Cavalheiro GL, Almeida MF, Pereira AA, Andrade AO (2009) Study of age-related changes in postural control during quiet standing through linear discriminant analysis. BioMed Eng 8(1):35. https://doi.org/10.1186/1475-925x-8-35 (ISSN 1475-925X)

Chester VL, Biden EN, Tingley M (2005) Gait analysis. Biomed Instrum Technol 39(1):64–74 [ISSN 0899-8205 (Print)]

Djuric-Jovicic M, Jovicic NS, Milovanovic I, Radovanovic S, Kresojevic N, Popovic MB (2010) Classification of walking patterns in Parkinson's disease patients based on inertial sensor data. In: 10th symposium on neural network applications in electrical engineering, Belgrade, Serbia, pp 3–6. https://doi.org/10.1109/NEUREL.2010.5644040

Felipe VP, Okut H, Gianola D, Silva MA, Rosa GJ (2014) Effect of genotype imputation on genome-enabled prediction of complex traits: an empirical study with mice data. BMC Genet 15:149. https://doi.org/10.1186/s12863-014-0149-9 (ISSN 1471-2156)

Fraiwan L, Khnouf R, Mashagbeh AR (2016) Parkinson's disease hand tremor detection system for mobile application. J Med Eng Technol 40(3):127–134. https://doi.org/10.3109/03091902.2016.1148792 (ISSN 0309-1902)

Fregni F, Boggio PS, Santos MC, Lima M, Vieira AL, Rigonatti SP, Silva MT, Barbosa ER, Nitsche MA (2006) Noninvasive cortical stimulation with transcranial direct current stimulation in Parkinson's disease. Mov Disord 21(10):1693–1702. https://doi.org/10.1002/mds.21012 [ISSN 0885-3185 (Print)]

Hadoush H, Al-Jarrah M, Khalil H, Al-Sharman A, Al-Ghazawi S (2018) Bilateral anodal transcranial direct current stimulation effect on balance and fearing of fall in patient with Parkinson's disease. NeuroRehabilitation 42(1):63–68. https://doi.org/10.3233/nre-172212 (ISSN 1053-8135)

Hoehn MM, Yahr MD et al (1998) Parkinsonism: onset, progression, and mortality. Neurology 50(2):318–318

Juen J, Cheng Q, Prieto-Centurion V, Krishnan JA, Schatz B (2014) Health monitors for chronic disease by gait analysis with mobile phones. Telemed J e-Health 20(11):1035–1041. https://doi.org/10.1089/tmj.2014.0025 (ISSN 1530-5627, 1556-3669)

Kermani BG, Schiffman SS, Nagle HT (2005) Performance of the Levenberg–Marquardt neural network training method in electronic nose applications. Sens Actuators B Chem 110(1):13–22

Krogh A (2008) What are artificial neural networks? Nat Biotechnol 26(2):195–7. https://doi.org/10.1038/nbt1386 (ISSN 1087-0156)

Lattari E, Costa SS, Campos C, de Oliveira AJ, Machado S, Neto GA (2017) Can transcranial direct current stimulation on the dorsolateral prefrontal cortex improves balance and functional mobility in Parkinson's disease? Neurosci Lett 636:165–169. https://doi.org/10.1016/j.neulet.2016.11.019 (ISSN 0304-3940)

Lee SH, Lim JS (2012) Parkinsons disease classification using gait characteristics and wavelet-based feature extraction. Expert Syst Appl 39(8):7338–7344. https://doi.org/10.1016/j.eswa.2012.01.084 (ISSN 0957-4174)

Lera G, Pinzolas M (2002) Neighborhood based Levenberg–Marquardt algorithm for neural network training. IEEE Trans Neural Netw 13(5):1200–1203

Li S, Da Xu L, Zhao S (2015) The internet of things: a survey. Inf Syst Front 17(2):243–259. https://doi.org/10.1007/s10796-014-9492-7 (ISSN 1572-9419)

Lilly JM, Olhede SC (2009) Higher-order properties of analytic wavelets. Trans Signal Proc 57(1):146–160. https://doi.org/10.1109/TSP.2008.2007607 (ISSN 1053-587X)

Lilly JM, Olhede SC (2012) Generalized Morse wavelets as a superfamily of analytic wavelets. IEEE Trans Signal Process 60:6036–6041

Lweesy K, Fraiwan L, Khasawneh N, Dickhaus H (2011) New automated detection method of OSA based on artificial neural networks using p-wave shape and time changes. J Med Syst 35(4):723–34. https://doi.org/10.1007/s10916-009-9409-z [ISSN 0148-5598 (Print)]

Manap HH, Md Tahir N, Yassin AIM (2011) Statistical analysis of Parkinson disease gait classification using artificial neural network. In: 2011 IEEE international symposium on signal processing and information technology (ISSPIT), Bilbao, Spain, pp 060–065. https://doi.org/10.1109/ISSPIT.2011.6151536 (ISBN 2162-7843)

MathWorks (2018) Morse wavelets. https://www.mathworks.com/help/wavelet/ug/morse-wavelets.html. Accessed 2 July 2018

Muro-De-La-Herran A, Garcia-Zapirain B, Mendez-Zorrilla A (2014) Gait analysis methods: an overview of wearable and non-wearable systems, highlighting clinical applications. Sensors (Basel) 14(2):3362–3394. https://doi.org/10.3390/s140203362 (ISSN 1424-8220)

Ngia LSH, Sjoberg J (2000) Efficient training of neural nets for nonlinear adaptive filtering using a recursive Levenberg–Marquardt algorithm. IEEE Trans Signal Process 48(7):1915–1927

Okut H, Gianola D, Rosa GJ, Weigel KA (2011) Prediction of body mass index in mice using dense molecular markers and a regularized neural network. Genet Res (Camb) 93(3):189–201. https://doi.org/10.1017/s0016672310000662 (ISSN 0016-6723)

Olhede SC, Walden AT (2002) Generalized morse wavelets. Trans Signal Proc 50(11):2661–2670. https://doi.org/10.1109/TSP.2002.804066 (ISSN 1053-587X)

Pachori RB, Hewson D, Snoussi H, Duchene J (2009) Postural time-series analysis using empirical mode decomposition and second-order difference plots. In: 2009 IEEE international conference on acoustics, speech and signal processing, Taipei, Taiwan, pp 537–540. https://doi.org/10.1109/ICASSP.2009.4959639 (ISBN 1520-6149)

Partridge D, Rae S, Wang WJ (1999) Artificial neural networks. J R Soc Med 92(7):385–385 (ISSN 0141-0768)

Perumal SV, Sankar R (2016) Gait monitoring system for patients with Parkinson's disease using wearable sensors. In: 2016 IEEE healthcare innovation point-of-care technologies conference (HI-POCT), Cancun, Mexico, pp 21–24. https://doi.org/10.1109/HIC.2016.7797687.

PhysioNet (2018) https://physionet.org/pn3/gaitpdb/. Accessed 10 May 2018

Prabhu P, Karunakar AK, Anitha H, Pradhan N(2018) Classification of gait signals into different neurodegenerative diseases using statistical analysis and recurrence quantification analysis. Pattern Recognit Lett.https://doi.org/10.1016/j.patrec.2018.05.006

Prieto TE, Myklebust JB, Hoffmann RG, Lovett EG, Myklebust BM (1996) Measures of postural steadiness: differences between healthy young and elderly adults. IEEE Trans Biomed Eng 43(9):956–66. https://doi.org/10.1109/10.532130 [ISSN 0018-9294 (Print)]

Qiao W, Sun HH, Chey WY, Lee KY (1998) Continuous wavelet analysis as an aid in the representation and interpretation of electrogastrographic signals. Ann Biomed Eng 26(6):1072–1081

Rovini E, Maremmani C, Cavallo F (2017) How wearable sensors can support Parkinson's disease diagnosis and treatment: a systematic review. Front Neurosci 11:555. https://doi.org/10.3389/fnins.2017.00555**(ISSN 1662-4548)**

Svozil D, Kvasnicka V, Pospichal J (1997) Introduction to multilayer feed-forward neural networks. Chemom Intell Lab Syst 39(1):43–62. https://doi.org/10.1016/S0169-7439(97)00061-0**(ISSN 0169-7439)**

Tadano S, Takeda R, Miyagawa H (2013) Three dimensional gait analysis using wearable acceleration and gyro sensors based on quaternion calculations. Sensors 13(7):9321. http://www.mdpi.com/1424-8220/13/7/9321**(ISSN 1424-8220)**

Tao W, Liu T, Zheng R, Feng H (2012) Gait analysis using wearable sensors. Sensors (Basel) 12(2):2255–2283. https://doi.org/10.3390/s120202255**(ISSN 1424-8220)**

The Parkinson Association (2018) https://www.parkinsonassociation.org/facts-about-parkinsons-disease/. Accessed 10 May 2018

Thuraisingham RA, Tran Y, Boord P, Craig A (2007) Analysis of eyes open, eye closed EEG signals using second-order difference plot. Med Biol Eng Comput 45(12):1243–9. https://doi.org/10.1007/s11517-007-0268-9**[ISSN 0140-0118 (Print)]**

Wang X (2015) The architecture design of the wearable health monitoring system based on internet of things technology. Int J Grid Util Comput 6(3/4):207–212. https://doi.org/10.1504/IJGUC.2015.070681**(ISSN 1741-847X)**

Weiss MJ, Moran MF, Parker ME, Foley JT (2013) Gait analysis of teenagers and young adults diagnosed with autism and severe verbal communication disorders. Front Integr Neurosci 7:33. https://doi.org/10.3389/fnint.2013.00033**(ISSN 1662-5145)**

Whittle MW (1996) Clinical gait analysis: a review. Hum Mov Sci 15(3):369–387

Yogev G, Giladi N, Peretz C, Springer S, Simon ES, Hausdorff JM (2005) Dual tasking, gait rhythmicity, and Parkinson's disease: which aspects of gait are attention demanding? Eur J Neurosci 22(5):1248–56. https://doi.org/10.1111/j.1460-9568.2005.04298.x [ISSN 0953-816X (Print)]

Zhang Y, Ogunbona PO, Li W, Munro B, Wallace GG (2013) Pathological gait detection of Parkinson's disease using sparse representation. In: 2013 international conference on digital image computing: techniques and applications (DICTA), Hobart, TAS, Australia, pp 1–8. https://doi.org/10.1109/DICTA.2013.6691510

Zhu S, Yang X (2015) Protecting data in cloud environment with attribute-based encryption. Int J Grid Util Comput 6(2):91–97. https://doi.org/10.1504/IJGUC.2015.068824**(ISSN 1741-847X)**